GH-releasing hormone promotes survival and prevents TNF-α-induced apoptosis and atrophy in C2C12 myotubes

(Article begins on next page)

17 July 2024

GH-Releasing Hormone Promotes Survival and Prevents TNF-α-Induced Apoptosis and Atrophy in C2C12 Myotubes

Davide Gallo, Iacopo Gesmundo, Letizia Trovato, Giulia Pera, Eleonora Gargantini, Marco Alessandro Minetto, Ezio Ghigo, Riccarda Granata

Abstract

Skeletal muscle atrophy is a consequence of different chronic diseases, including cancer, heart failure, and diabetes, and also occurs in aging and genetic myopathies. It results from an imbalance between anabolic and catabolic processes, and inflammatory cytokines, such as TNF-α, have been found elevated in muscle atrophy and implicated in its pathogenesis. GHRH, in addition to stimulating GH secretion from the pituitary, exerts survival and antiapoptotic effects in different cell types. Moreover, we and others have recently shown that GHRH displays antiapoptotic effects in isolated cardiac myocytes and protects the isolated heart from ischemia/reperfusion injury and myocardial infarction in vivo. On these bases, we investigated the effects of GHRH on survival and apoptosis of TNF-α-treated C2C12 myotubes along with the underlying mechanisms. GHRH increased myotube survival and prevented TNF-α-induced apoptosis through GHRH receptor-mediated mechanisms. These effects involved activation of phosphoinositide 3-kinase/Akt pathway and inactivation of glycogen synthase kinase-3β, whereas mammalian target of rapamycin was unaffected. GHRH also increased the expression of myosin heavy chain and the myogenic transcription factor myogenin, which were both reduced by the cytokine. Furthermore, GHRH inhibited TNF-α-induced expression of nuclear factor-κB, calpain, and muscle ring finger1, which are all involved in muscle protein degradation. In summary, these results indicate that GHRH exerts survival and antiapoptotic effects in skeletal muscle cells through the activation of anabolic pathways and the inhibition of proteolytic routes. Overall, our findings suggest a novel therapeutic role for GHRH in the treatment of muscle atrophy-associated diseases.

Skeletal muscle atrophy, or wasting, is a debilitating consequence of different chronic diseases, including cancer, heart failure, diabetes, rheumatoid arthritis, and AIDS. It also occurs in aging, muscle disuse, and starvation as well as in genetic myopathies, including muscle dystrophies, which lead to muscle fiber degeneration and loss of muscle mass. Muscle atrophy results from an imbalance between anabolic and catabolic processes; indeed, in addition to other mechanisms, it is primarily caused by hyperactivation of the main cellular degradation pathways, including the ubiquitin-proteasome system (UPS) and the autophagy-lysosome pathway (1–3).

Several cytokines, such as TNF-α, IL-1β, and interferon-γ (IFN-γ), have been implicated in the pathogenesis of muscle wasting. In particular, TNF-α has been shown to be elevated in conditions that lead to muscle atrophy (1–3). Furthermore, TNF-α is a potent trigger of muscle wasting in vitro and in vivo, through the inhibition of myogenesis and induction of apoptosis and proteolysis, via the activation of nuclear factor-κB (NF-κB) and different components of the UPS (4–7). In contrast to other diseases, there are currently no effective and safe medicines to treat muscle atrophy associated with different disorders. Therefore, the identification of compounds able to activate anabolic pathways and to counteract those involved in muscle degeneration would be essential for designing new therapeutic approaches to reduce muscle wasting.

The hypothalamic hormone GHRH is known for its stimulatory effects on pituitary GH synthesis and release and somatotrope expansion (8). Furthermore, extrahypothalamic GHRH has been implicated in many peripheral actions, via autocrine/paracrine mechanisms, and exogenous GHRH also regulates proliferation, survival, apoptosis, differentiation, and wound healing in different tissues and cell types (9). GHRH effects involve binding to GHRH receptor (GHRH-R), whose activation stimulates adenylyl cyclase/cAMP/protein kinase A via Gαs subunit (10). Alternatively, GHRH stimulates the Ras/MAPK via βγ-subunits, to promote cell growth (11).

We have recently demonstrated that GHRH displays antiapoptotic effects in isolated cardiac myocytes through GHRH-R-mediated mechanisms and activation of phosphoinositide-3 kinase (PI3K)/Akt and ERK1/2 (12). GHRH also improves heart function and reduces infarct size in isolated rat hearts subjected to ischemia/reperfusion, either when administered before ischemia (12) or during early reperfusion (13). These effects involved activation of reperfusion injury salvage kinases, PI3K/Akt, ERK1/2, and glycogen synthase kinase-3β (GSK-3β), and survivor activating factor enhancement pathway, such as signal transducer and activator of transcription-3. Other groups have shown that GHRH agonists improved cardiac performance and decreased infarct size in vivo after myocardial infarction (14, 15) and chronic cardiac injury (16), via GH/IGF-1-independent and GHRH-R-dependent mechanisms. Recently a role on cardiac stem cell proliferation and survival has been also demonstrated (17).

In addition to cardiac myocytes, the role of GHRH in other muscle cells has not been investigated. Notably, in line with GHRH-induced signaling in cardiac myocytes, activation of PI3K/Akt/mammalian target of rapamycin (mTOR) pathway by growth factors such as IGF-1 has been shown to act as a positive regulator of muscle growth and to suppresses catabolic pathways and prevent muscle atrophy (1–3, 18). Therefore, based on the above findings, we hypothesized that GHRH would promote survival and prevent atrophy of skeletal muscle cells. To verify this hypothesis, GHRH effects were assessed on survival and apoptosis of C2C12 myotubes, treated with TNF-α either during the myogenic process or at the end of differentiation. The underlying signaling pathways were also investigated along with the major mechanisms involved in muscle cell degeneration and atrophy.

Materials and Methods
Reagents

Mouse GHRH and JV-1–36 were from Phoenix Pharmaceuticals. DMEM, newborn calf serum, horse serum, Fungizone, penicillin/streptomycin, trypsin, and AlexaFluor 594 antibodies were purchased from Life Technologies (Invitrogen). GHRH, total p70 ribosomal S6 kinase (p70S6K), myosin heavy chain (MyHC), actin, total GSK-3β, and Bcl-2 antibodies were from Santa Cruz Biotechnology (DBA). TNF-α, 3-(4,5-dimethylthiazol-2-yl)-2,5-diphenyltetrazolium bromide (MTT), BSA, Hoechst 33258, wortmannin, rapamycin, and the mammalian cell lysis kit were from Sigma-Aldrich. Phosphorylated (P)-Akt (S473), P-NF-κ B p65 (S536), total antibodies, GHRH-R, calpain, myogenin, and muscle ring finger 1 (MuRF1) were from Abcam. P-p70S6K (Thr389) and P-GSK-3β (Ser9) were from Cell Signaling Technology (EuroClone, Pero). Horseradish peroxidase-conjugated secondary antibodies were provided by Bethyl Laboratories (TemaRicerca). RT-PCR reagents were from Life Technologies. The specificity and sensitivity of all the antibodies were tested and guaranteed as indicated in the manufacturer's data sheets (see Table 1).

Table 1. Antibodies

Peptide/Protein Target	Name of Antibody	Manufacturer, Catalog Number	Species Raised (Monoclonal or Polyclonal)	Dilution Used
NF-κB p65	Anti-NF-κB p65 antibody	Abcam, Ab31481	Rabbit, polyclonal	1:500
NF-κB p65 (phospho-S536)	Anti-NF-κB p65 (phospho-S536) antibody	Abcam, Ab131109	Rabbit, polyclonal	1:500
Phospho-p70S6K (Thr389)	Phospho-p70S6K (Thr389) antibody	Cell Signaling Technology, 9205	Rabbit, polyclonal	1:1000
p70S6Kα (H-9)	p70S6Kα (H-9) antibody	Santa Cruz Biotechnology, sc-8418	Mouse, monoclonal	1:500
Calpain S1	Rabbit monoclonal (EPR3324) to calpain S1 antibody	Abcam, Ab92333	Rabbit, monoclonal	1:3000
GHRH (H-20)	GHRH (H-20) antibody	Santa Cruz Biotechnology, sc-10285	Goat, polyclonal	1:500
GHRH-R	Anti-GHRH-R antibody	Abcam, Ab28692	Rabbit, polyclonal	1:2000

Peptide/Protein Target	Name of Antibody	Manufacturer, Catalog Number	Species Raised (Monoclonal or Polyclonal)	Dilution Used
Myogenin	Antimyogenin antibody	Abcam, Ab124800	Rabbit, monoclonal	1:500
MyHC	MYH7 (K-13)	Santa Cruz Biotechnology, sc-168678	Goat, polyclonal	1:200
Actin	Actin (H-6) antibody	Santa Cruz Biotechnology, sc-376421	Mouse, monoclonal	1:300
Phospho-GSK-3β (Ser9)	Phospho-GSK-3β (Ser9) antibody	Cell Signaling Technology, 9336	Rabbit, polyclonal	1:2000
GSK-3β (H-76)	GSK-3β (H-76) antibody	Santa Cruz Biotechnology, 9166	Rabbit, polyclonal	1:1000
P-Akt (S473)	Anti-AKT1 (phospho-S473) antibody	Abcam, Ab66138	Rabbit, polyclonal	1:500
AKT	Anti-pan-AKT antibody	Abcam, Ab8805	Rabbit, polyclonal	1:500
MuRF1	Anti-MURF1 antibody	Abcam, Ab77577	Rabbit, polyclonal	1:500
Bcl-2	Bcl-2 (DC 21) antibody	Santa Cruz Biotechnology, sc-783	Rabbit, polyclonal	1:500
Alexa Fluor 594	Alexa Fluor 594 rabbit antigoat IgG (H + L)	Life Technologies, A-11080	Rabbit, antigoat	1:450

Cell culture and treatments

The mouse myoblast cell line C2C12 was obtained from IZSLER (Istituto Zooprofilattico Sperimentale della Lombardia e dell'Emilia, Brescia, Italy). Undifferentiated myoblasts were maintained at subconfluent density at 37ºC in a 5% CO_2 humidified atmosphere in DMEM with 10% newborn calf serum, 1% penicillin-streptomycin, and 0.5% Fungizone. To induce differentiation, confluent cells were shifted to a differentiation medium (DM) containing DMEM supplemented with 2% heat-inactivated horse serum, and the medium was changed every 48 hours. Myogenic differentiation of C2C12 myotubes was assessed after 6 days in DM by observation of cell morphology under a phase-contrast microscopy. For experiments in differentiating myoblasts, confluent C2C12 myoblasts were incubated in DM with the different stimuli, from the beginning of the differentiation protocol up to 6 days; stimuli were added every 48 hours at the medium change. For experiments in myotubes, cells were differentiated for 4 days and then incubated with the different stimuli for further 48 hours.

Reverse transcription-polymerase chain reaction

Total RNA was extracted from C2C12 cells, mouse male brain, and soleus muscle, obtained as previously described (19); human rectus abdominis muscle; and LnCaP human prostate cancer cells. Reverse transcription to cDNA from 3 μg RNA was performed as previously described (12). The primer sequences for mouse GHRH-R were as follows: forward, 5'-CCAAACCAGCTTTCTGGTGGC-3'; reverse, 5'-GGCCTAGCACTCAGAGGT-3' (NM_001003685.3). The product of the first amplification was 563 bp. Next, a second PCR (40 cycles) was performed on 9 μL of the primary PCR products. The primers, designed using Primer3 Output, spanned the first amplification product and were forward, 5'-CGGCTTTCCAAATCAACACT-3' and reverse, 5'-ACCATTTGCGTGAAATCTCC-3' (L01407). Mouse GHRH primers, obtained with Primer3, were as follows: forward, 5'-TGTGATCCTCATCCTCACCA-3' and reverse, 5'-ATCCTCTCCCCTTGCTTGTT-3' (NM_01028 5.2). Primers for 18S rRNA were as follows: forward, 5'-GTGGAGCGATTTGTCTGGTT-3' and reverse, 5'-CGCTGAGCCAGTTCAGTGTA-3' (NR_046237.1). Nine microliters of cDNA were amplified with GeneAmp PCR system (PerkinElmer) in 50 μL in the following conditions: 94ºC for 30 seconds, annealing for 30 seconds (59ºC and 52ºC for the first and second GHRH-R PCR, respectively; 56ºC for the GHRH PCR); and 72ºC for 30 seconds, 72ºC for 7 minutes. The final PCR products (199 bp for GHRH-R, 171 bp for GHRH and 201 bp for 18S rRNA) were separated by 1.8% agarose gel electrophoresis and visualized by ethidium bromide staining. Mouse brain was used as the positive control; the negative control consisted of buffer alone with no RNA. 18S rRNA amplification served as internal control.

RT-PCR for human GHRH-R and GHRH was performed using the following primers: GHRH-R (obtained with Primer3) forward, 5'-CCTACTGCCCTTAGGATGCTGG-3', reverse, 5'-GCCATGCCACTTCCGTGAGAT-3' for the first PCR (annealing 62 C) (XM_011515263.1), and forward, 5'-GCACCTTTGAAGCCAGAGAAGG-3', reverse, 5'-CACGTGCCAGTGAAGAGCACGG-3' for the second PCR (annealing 64ºC) (AF282260); GHRH, forward, 5'-AATTGGAGAGCATCCTGGTG-3', reverse, 5'-ACCGGTATGGGGGAATTTTA-3' (NM_021081), as previously described (20). The amplification products were 523 bp for GHRH-R and 175 bp for GHRH. The LnCaP human prostate cancer cell line (obtained from American Type Culture Collection, LGC Standards Srl) was used as positive control.

Survival assay

C2C12 myoblasts were seeded on 96-well plates at a density of 5×10^3 cells per well and then differentiated as described above. After incubation with the different stimuli, MTT, 5 mg/mL in PBS solution, was added and cells incubated at 37ºC for 1 hour. The newly formed formazan crystals were dissolved in 100 µL/well of dimethylsulfoxide. The absorbance of solubilized formazan was read at 570 nm using a 96-well plate reader (SorinBiomedica, ETI-Fast Reader), as previously described (21).

Apoptosis assay

Morphological changes in the nuclei of apoptotic cells were detected by Hoechst 33258 staining. C2C12 myoblasts were seeded in 24-well plates on glass coverslips, differentiated, and treated as described (12). After incubation, cells were washed twice with ice-cold PBS, fixed with 4% formaldehyde for 15 minutes at 4ºC, washed again, and stored at −20ºC in 70% ethanol until use. Cells were then washed twice in PBS and stained in 300 µL PBS containing 10 µg/mL Hoechst 33258. After 15 minutes of incubation at room temperature, coverslips were mounted on glass slides using fluorescent mounting medium, and 500 stained nuclei were double counted under a 4',6'-diamino-2-phenylindole filter-equipped fluorescence microscope.

Western blotting

Western blotting was performed as described (21). Proteins (40–50 µg) were separated by SDS-PAGE using 8%–13% gels, transferred to nitrocellulose membranes (Bio-Rad Laboratories), and then incubated with the specific antibodies (Bcl-2, P-Akt, P-GSK-3β, P-p70S6K, myogenin, P-NF-κB, MuRF1, and calpain). Blots were reprobed with the respective total antibodies or α-actin (for calpain, myogenin, and MuRF1) for protein normalization. Immunoreactivity was visualized using horseradish peroxidase-conjugated antirabbit antibodies by enhanced chemiluminescence (Bio-Rad Laboratories), processed by ChemiDoc XRS (Bio-Rad Laboratories) and densitometric analysis was performed with Quantity One software (Bio-Rad Laboratories).

Immunostaining for MyHC and myogenic index of fusion

Cells were grown and differentiated in 24-well plates on glass coverslips for 4 days and then incubated with GHRH 0.5 µM alone or with TNF-α 20 ng/mL for a further 48 hours. Cells were then washed twice with ice-cold PBS, fixed with 4% paraformaldehyde for 20 minutes in ice, permeabilized, incubated with PBS-2% normal goat serum for 1 hour, and stained with anti-MyHC antibody overnight at 4ºC. After washing with PBS, cells were incubated with goat antirabbit Alexa Fluor 594 (1:400 dilution in PBS-2% normal goat serum) for 1 hour in the dark and then nuclei counterstained with Hoechst 33258. The cover slips were mounted on glass slides using fluorescent mounting medium (Dako) and analyzed under an inverted fluorescence microscope. Red and blue channels were assigned to MyHC and nuclei, respectively. Images from Hoechst-stained nuclei (blue) and MyHC (red) were taken using a Leica DM2000 fluorescent microscope and a Leica DFC340FX camera, and analysis was performed with a Leica Suite image analysis software. The myogenic index of fusion was calculated to assess the number of formed myotubes. The total number of Hoechst-stained nuclei and the number of nuclei contained within the bright red-stained area

(MyHC positive) were counted using 10 randomly chosen microscopic fields from three independent experiments. The myogenic index was then calculated as the percentage of nuclei incorporated into the syncytium (defined as containing at least two nuclei) in relation to the overall number of nuclei.

Statistical analysis

Results are presented as means ± SE. Results were analyzed using a two-tailed Student t test or a two-way ANOVA followed by Tukey honestly significant difference for post-ANOVA comparisons (GraphPad Prism 5.0 Software Inc). Significance was established at $P < .05$.

Results
GHRH-R and GHRH expression during differentiation of C2C12 myoblasts

GHRH-R and GHRH mRNA expression was assessed in C2C12 myoblasts, from day 0 to day 6 of differentiation, when they become fully differentiated myotubes. To induce myogenesis, growth medium was replaced with DM, as described in *Materials and Methods*. Under these conditions, C2C12 myoblasts exit the cell cycle, differentiate, and fuse into multinucleated skeletal myotubes expressing contractile proteins (22). Myotube formation was confirmed at day 6 by phase-contrast microscopy morphological evaluation (Figure 1A). GHRH-R mRNA was found expressed in myoblasts (day 0) and increased at day 3, remaining constant up to day 6 in myotubes (Figure 1B). Conversely, GHRH mRNA, which was also present at day 0, showed no variation during differentiation (Figure 1C). Analysis for the GHRH-R splice variant-1 was also performed by nested PCR, showing no expression in myoblasts and myotubes (data not shown). As for mRNA, GHRH-R protein increased at days 3 and 6, compared with day 0 (Figure 1D). Moreover, GHRH protein levels progressively increased at days 3 and 6, differently from what was observed for the mRNA (Figure 1D). These results indicate that C2C12 skeletal muscle cells express both GHRH and its receptor during differentiation of myoblasts into myotubes. Mouse and human skeletal muscle was also examined and both GHRH-R and GHRH mRNA were found expressed in mouse soleus muscle (Figure 1E) and in human rectus abdominis muscle (Figure 1F).

Figure 1. GHRH and GHRH-R expression during C2C12 myoblast differentiation.
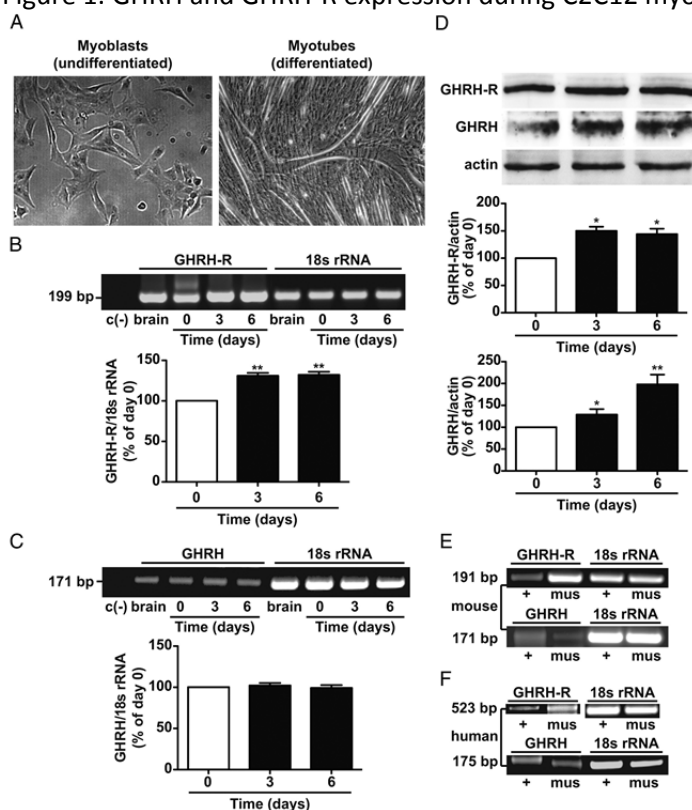
A, Representative images (phase contrast microscopy, ×200) of C2C12 cell differentiation. Myoblasts (left panel) were induced to differentiate for 6 days into myotubes (right panel). GHRH-R (B) and GHRH (C) mRNA expression assessed by RT-PCR in in C2C12 cells either undifferentiated (day 0) or during the indicated days of differentiation. Buffer alone was used as negative control (c−). Mouse brain was used as positive control and 18S rRNA amplification as internal control. Results, normalized to 18S rRNA transcript, are expressed as percentage of day 0 and are the mean ± SE from three independent experiments. **, $P < .01$ vs day 0. D, Western blot analysis for GHRH-R (upper panel) and GHRH (middle panel), assessed at the indicated days of differentiation. Equal protein loading was determined by reprobing with antibody to actin (lower panel). Graph represents the densitometric analysis of either GHRH-R or GHRH normalized to actin and reported as percentage of day 0. *, $P < .05$, **, $P < .01$ vs day 0 (n = 3). E, GHRH-R and GHRH mRNA expression assessed by RT-PCR in mouse soleus muscle. Mouse brain was used as positive control. F, GHRH-R and GHRH mRNA in human rectus abdominis muscle. The LnCaP human prostate cancer cell line was used as positive control. 18S rRNA amplification served as internal control for both E and F.

GHRH promotes cell survival and inhibits TNF-α-induced apoptosis in differentiating myoblasts

TNF-α induces skeletal muscle wasting in different chronic diseases by inducing apoptosis of muscle fibers (3, 23). Furthermore, high concentrations of TNF-α have been shown to reversibly inhibit myotube formation in vitro (6, 24, 25). To examine GHRH effect on C2C12 cell survival and apoptosis, different concentrations of the hormone were tested (0.001–0.5 μM), either alone or in combination with TNF-α (10 and 20 ng/mL), during differentiation. C2C12 myoblasts were cultured in DM for up to 6 days and exposed to both TNF-α and GHRH every 48 hours. Cell survival and apoptosis were assessed at day 6, in differentiated myotubes. GHRH alone slightly but significantly increased cell survival in DM (control) at the highest concentration tested (0.5 μM), having no effect at the lowest concentrations (EC$_{50}$: 399 nM). TNF-α reduced cell survival at 10 ng/mL and, to a greater extent, at 20 ng/mL, as compared with control, whereas GHRH dose dependently inhibited this effect, at both TNF-α concentrations (Figure 2A). Similar effects were obtained for apoptosis, assessed by Hoechst 33258 staining of apoptotic nuclei. GHRH per se moderately reduced apoptosis in DM and also dose dependently blunted the proapoptotic effect of TNF-α at both 10 and 20 ng/mL (Figure 2B). Next, to assess GHRH-R involvement in GHRH survival and antiapoptotic effects, different concentrations of the GHRH antagonist JV-1–36 (12, 26) were given to differentiating C2C12 cells, in either the absence or presence of GHRH (0.5 μM). As expected, GHRH increased cell survival and reduced apoptosis, compared with control. JV-1–36 reduced cell survival at 0.5 μM, but not at 0.001 and 0.01 μM, and blocked GHRH-induced survival at all the concentrations tested (Figure 2C) (EC$_{50}$: 293 nM). JV-1–36 also increased apoptosis at both 0.01 and 0.5 μM and blocked GHRH antiapoptotic action at these concentrations but not at 0.001 μM, in which it showed no effect, even per se (Figure 2D). Based on these results, GHRH 0.5 μM, TNF-α 20 ng/mL, and JV-1–36 0.1 μM were chosen as best concentrations for the subsequent studies. The GHRH ability to counteract TNF-α harmful effects in differentiating myotubes was then assessed in the presence of JV-1–36. JV-1–36 blocked the survival and antiapoptotic effects of GHRH, in both the absence and presence of TNF-α (Figure 2, E and F). Collectively these results suggest that GHRH displays survival and antiapoptotic effects in myotubes exposed to TNF-α during differentiation through GHRH-R-mediated mechanisms.

Figure 2. Survival and antiapoptotic effects of GHRH assessed in C2C12 myotubes treated with TNF-α during differentiation.
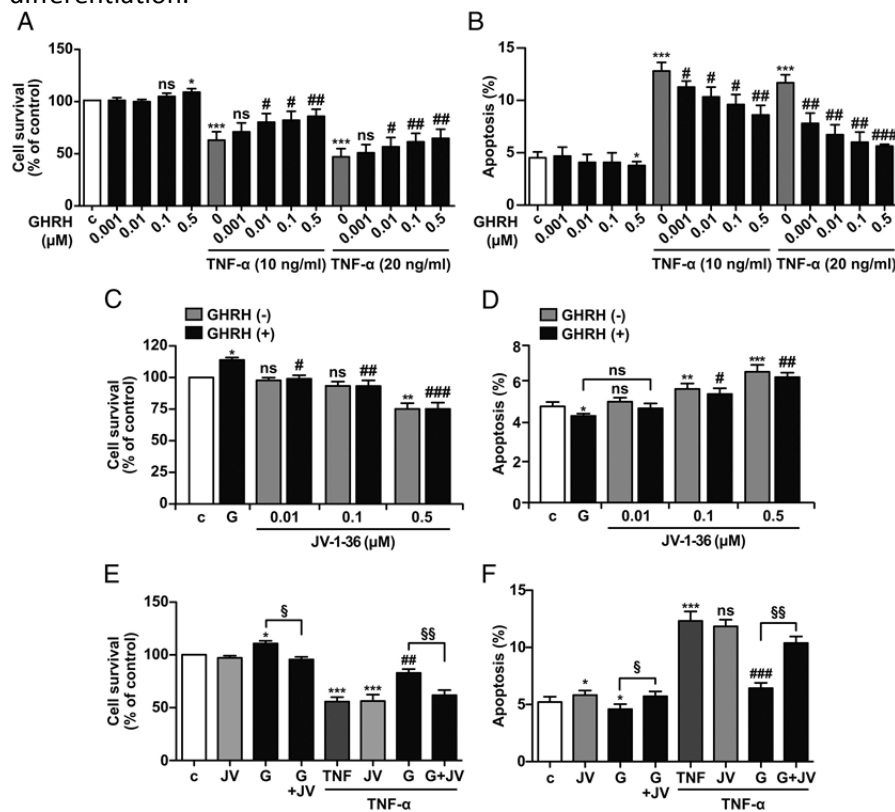
The cells were exposed to both TNF-α and GHRH every 48 hours (from day 0 to 6). Cell survival and apoptosis were assessed at day 6 by MTT and by counting fragmented/condensed Hoechst-stained nuclei, respectively. Survival (A) and antiapoptotic effects (B) of GHRH, used at the indicated concentrations, in cells cultured in DM, either alone (control) or with 10 ng/mL or 20 ng/mL TNF-α, are shown. Values are mean ± SE of three independent experiments. *, $P < .05$, **, $P < .01$, ***, $P < .001$ vs c; #, $P < .05$, ##, $P < .01$, ###, $P < .001$ vs each concentration of TNF-α alone (gray bars). Cell survival (C) and apoptosis (D) in cells cultured in DM, either without or with GHRH (G) (0.5 μM), and with JV-1–36, at the indicated concentrations are shown. *, $P < .05$, **$P < .01$, ***, $P < .001$ vs c (ns, not significant); #, $P < .05$, ##, $P < .01$, ###, $P < .001$ vs each concentration of GHRH alone (n = 3) (ns, not significant vs c). Cell survival (E) and apoptosis (F) in cells treated either with or without GHRH (G) (0.5 μM), JV-1–36 (0.1 μM), and TNF-α (20 ng/mL) are shown. *, $P < .05$, ***, $P < .001$ vs c; ##, $P < .01$, ###, $P < .001$ vs TNF-α alone (n = 3); §, $P < .05$, §§, $P < .01$. Apoptosis (B, D, and F) is expressed as a percentage of apoptotic cells obtained from duplicate determinations (500 cells each, n = 3).

GHRH promotes cell survival and inhibits TNF-α-induced apoptosis in differentiated myotubes

We next assessed the potential survival and antiapoptotic effects of GHRH in differentiated myotubes treated with TNF-α. C2C12 cells were induced to differentiate for 4 days in DM and then treated for a further 48 hours with either GHRH, TNF-α, or a combination of both. Cell survival, assessed by MTT, was reduced by TNF-α, with similar effects at 10 and 20 ng/mL. GHRH alone had no effect with respect to control; however, it counteracted TNF-α effects, particularly at the cytokine concentration of 20 ng/mL (Figure 3A). Similarly, TNF-α increased apoptosis at both 10 and even more at 20 ng/mL, and this effect was inhibited by GHRH, which reduced apoptosis even alone, with respect to control (Figure 3B). Furthermore, GHRH, which per se increased the antiapoptotic protein Bcl-2, also counteracted TNF-α-induced reduction of Bcl-2 (Figure 3C). Next, the role of GHRH-R on GHRH protective effects was assessed by incubating myotubes with different concentrations of JV-1–36, either alone or with GHRH. Figure 3D shows that, compared with control, cell survival was unaffected by JV-1–36 as well as by the combination of GHRH and JV-1–36. Conversely, JV-1–36 increased apoptosis at the highest concentration tested (0.5 μM) and blocked the antiapoptotic effect of all GHRH concentrations (Figure 3E). Based on these results, 0.1 μM JV-1–36 was used in the subsequent experiments. As expected, JV-1–36 had no effect on cell survival and apoptosis when administered alone or with TNF-α. However, it completely blocked both the survival and antiapoptotic effects of GHRH in TNF-α-treated cells (Figure 3, F and G). Furthermore, in addition to

reducing Bcl-2 expression alone, JV-1–36 also inhibited GHRH-induced Bcl-2 increase in cells treated with TNF-α (Figure 3H).

Figure 3. GHRH survival and antiapoptotic effects in C2C12 myotubes treated with TNF-α.
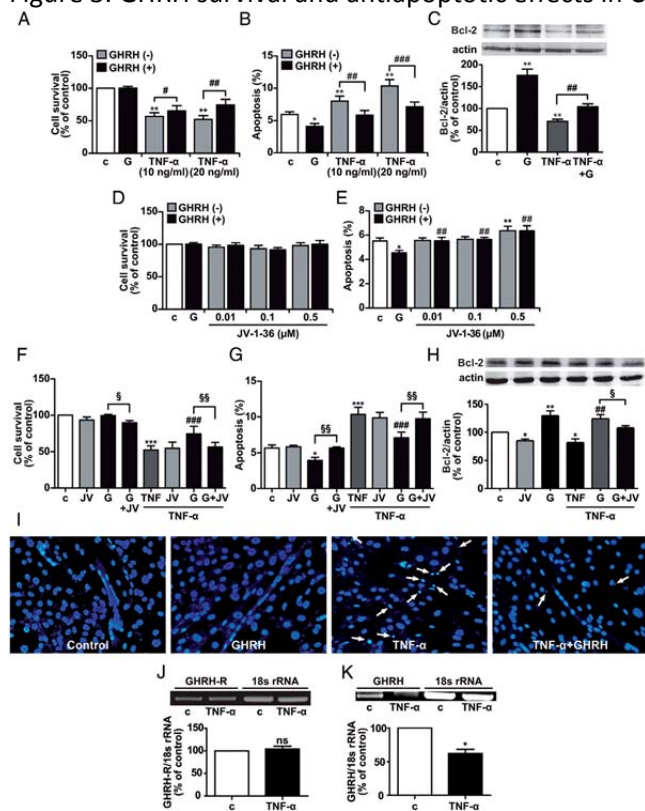
Cells were cultured in DM for 4 days and then for a further 48 hours in DM [control (c)] without or with TNF-α, GHRH (G) (0.5 μM), or JV-1–36, either alone or in combination. A, Cell survival assessed by MTT. B, Apoptosis evaluated by counting fragmented/condensed Hoechst-stained nuclei. For both panels A and B, *, *P* < .05, **, *P* < .01 vs c; #, *P* < .05, ##, *P* < .01, ###, *P* < .001. C, Bcl-2 protein expression (top panel) assessed by Western blot on whole lysates from myotubes either unstimulated [control (c)] or stimulated with GHRH (0.5 μM), TNF-α (20 ng/mL) or a combination of both for 48 hours. Equal protein loading was determined by reprobing with antibody to actin (bottom panel). Blots are representative of three independent experiments. Graphs show the densitometric analysis of Bcl-2 normalized to actin and reported as percentage of control. **, *P* < .01 vs c; ##, *P* < .01. Cell survival (D) and apoptosis (E) was assessed by Hoechst staining in myotubes both untreated [control (c)] or stimulated with the indicated concentrations of JV-1–36 and either without or with GHRH (0.5 μM). *, *P* < .05, **, *P* < .01 vs. c; ##, *P* < .01 vs GHRH (−), (n = 3). Cell survival (F) and apoptosis (G) in myotubes were treated either with or without GHRH (0.5 μM), JV-1–36 (0.1 μM), and TNF-α (20 ng/mL). **, *P* < .01, ***, *P* < .001 vs c; ###, *P* < .001 vs TNF-α alone (n = 3); §, *P* < .05, §§, *P* < .01. Apoptosis (B, E, and G) is expressed as a percentage of apoptotic cells from duplicate determinations (500 cells each, n = 3). H, Bcl-2 expression (top panel) assessed by Western blot on myotubes either untreated [control (c)] or treated with the indicated stimuli (0.1 μM JV-1–36, 0.5 μM GHRH, 20 ng/mL TNF-α) for 48 hours. Blots were reprobed with antibody to actin (bottom panel). *, *P* < .05, **, *P* < .01 vs c; ##, *P* < .01; §, *P* < .05. I, Hoechst 33258 nuclear immunofluorescence staining (original magnification, ×200) of C2C12 myotubes cultured for 48 hours in DM, either alone or with GHRH (0.5 μM), TNF-α (20 ng/mL), or a combination of both. Arrows, apoptotic cells. GHRH-R (J) and GHRH (K) mRNA expression is assessed by RT-PCR in myotubes treated with TNF-α (20 ng/mL) for 48 hours. Results, normalized to 18S rRNA transcript, are expressed as a percentage of control. *, *P* < .05; ns, not significant (n = 3). c, untreated cells.

Hoechst staining for apoptotic nuclei showed that TNF-α-treated cells appeared smaller, with many picnotic/condensed nuclei and unable to form multinucleated myotubes. These effects were counteracted by GHRH, which strongly reduced the number of apoptotic nuclei and preserved the myotubular structure (Figure 3I). As for differentiating myoblasts, these results suggest that GHRH counteracts the harmful effects of TNF-α in differentiated myotubes through receptor-mediated mechanisms.

Next, to assess whether TNF-α would influence GHRH-R and GHRH expression, RT-PCR was performed in C2C12 myotubes treated with TNF-α for 48 hours, from day 4 of differentiation. GHRH-R mRNA levels were

unchanged (Figure 3J), whereas GHRH expression was reduced in TNF-α-treated cells with respect to control (Figure 3K).

GHRH survival and antiapoptotic effects in myotubes involve phosphorylation of PI3K/Akt and GSK-3β but not mTOR

In addition to being a major survival and antiapoptotic pathway in most cell types (12, 27), PI3K/Akt plays a pivotal role in the control of skeletal muscle hypertrophy and atrophy (3). Downstream Akt targets include GSK-3β and mTOR, which are phosphorylated and thereby inhibited or activated, respectively. In C2C12 myotubes, GHRH increased the phosphorylation of Akt up to 90 minutes, with a decrease at 120 minutes, compared with the basal time point (Figure 4A). GSK3-β phosphorylation was also increased by GHRH, at 90 and, particularly, 120 minutes (Figure 4B). GHRH effect on Akt and GSK3-β phosphorylation was then assessed at 90 minutes in TNF-α-treated myotubes, either without or with the PI3K/Akt inhibitor wortmannin. GHRH alone increased both Akt (Figure 4C) and GSK3-β (Figure 4D) activation, with respect to untreated cells; furthermore, it counteracted the inhibitory effect of TNF-α on phosphorylation of both pathways. Wortmannin blocked GHRH-induced increase of both P-Akt and P-GSK3-β in TNF-α-treated cells but had no effect per se or with TNF-α only (Figure 4, C and D). Wortmannin also blocked GHRH survival and antiapoptotic effects in TNF-α-treated cells (Figure 4, E and F). Moreover, GHRH ability to counteract TNF-α-induced reduction of both Akt and GSK3-β phosphorylation was inhibited in myotubes preincubated with JV-1–36, whereas the GHRH antagonist alone had no effect with respect to control (Figure 4, G and H).

Figure 4. PI3K/Akt and GSK3-β signaling in GHRH survival and antiapoptotic effects.
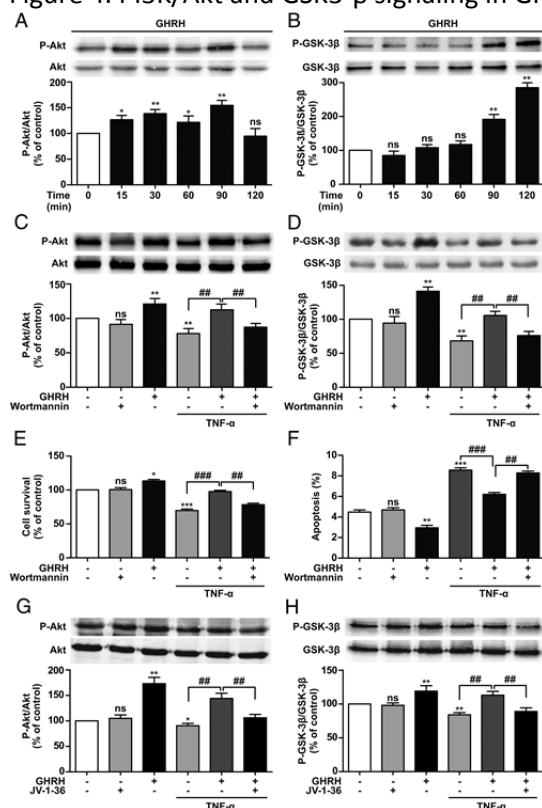
Conversely, GHRH had no effect on the mTOR downstream target p70S6K, either alone or in combination with TNF-α (Figure 5, A and B). Furthermore, rapamycin, a selective blocker of mTOR, did not prevent GHRH-induced survival in the presence of TNF-α (Figure 5C). These results suggest that GHRH survival effects in TNF-α-treated myotubes require the phosphorylation of PI3K/Akt and GSK3-β (activation and inhibition, respectively) but not of mTOR/p70S6K.

Figure 5. GHRH-induced survival in TNF-α-treated myotubes does not involve activation of mTOR/p706SK.
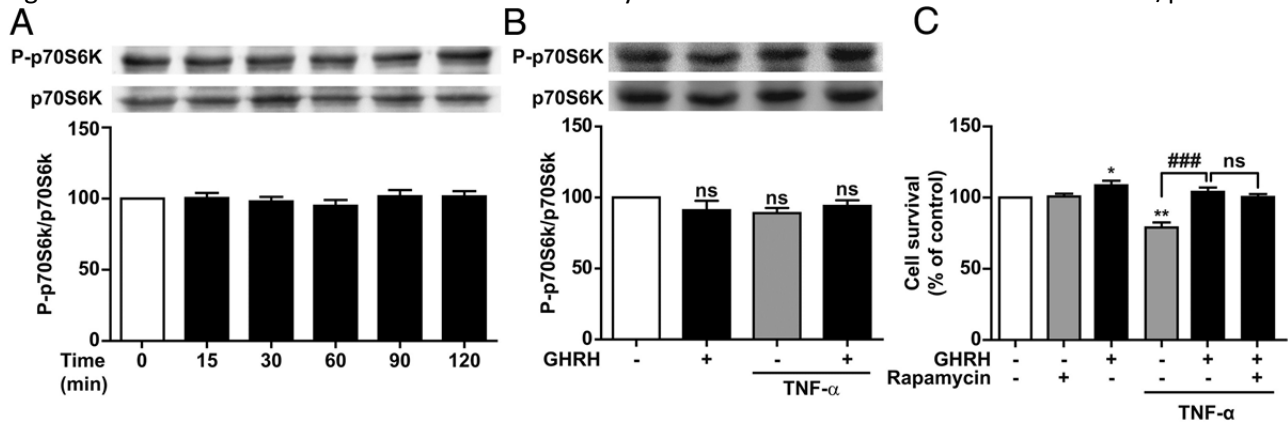
A, P70S6K phosphorylation assessed by Western blot on whole lysates from C2C12 myotubes stimulated with 0.5 μM GHRH for the indicated times (top panels). B, P70S6K phosphorylation in C2C12 cells differentiated for 4 days and then incubated for 90 minutes either with or without 0.5 μM GHRH and TNF-α (20 ng/ml). For both A and B, equal protein loading was determined by reprobing with antibodies to the respective total proteins (bottom panels). Blots are representative of three independent experiments. ns, not significant vs untreated cells (white column). C, Cell survival assessed by MTT in myotubes cultured in DM for 4 days and then for a further 48 hours without or with GHRH (0.5 μM), TNF-α (20 ng/mL), and rapamycin (0.05 μM), either alone or in combination. *, $P < .05$, **, $P < .01$ and vs untreated cells (white column); ###, $P < .001$ (n = 3).

GHRH counteracts TNF-α-induced myofibrillary protein degradation and activation of proteolytic pathways

Muscle wasting occurs when protein degradation exceeds protein synthesis and involves the dysregulation of myogenic regulatory factors and genes associated with myotube formation (1–3). GHRH effects in myotubes were first assessed on the regulation of MyHC, a major functional protein of adult skeletal muscle, which is degraded by TNF-α both in vitro and in vivo (7, 28). C2C12 cells were differentiated for 4 days and then treated for 48 hours with GHRH or TNF-α, alone or in combination. Myotube morphology was examined by immunofluorescence for MyHC. TNF-α markedly induced myotube degradation, compared with untreated cells, whereas coincubation with GHRH prevented this effect and restored myotube morphology and MyHC normal distribution (Figure 6A). Accordingly, results on myogenic index of fusion showed that TNF-α strongly reduced the myogenic index with respect to control. GHRH had no effect alone; however, it strongly counteracted TNF-α-induced decrease of MI (Figure 6B).

Figure 6. GHRH protective effects against TNF-α-induced protein degradation and activation of proteolytic pathways.
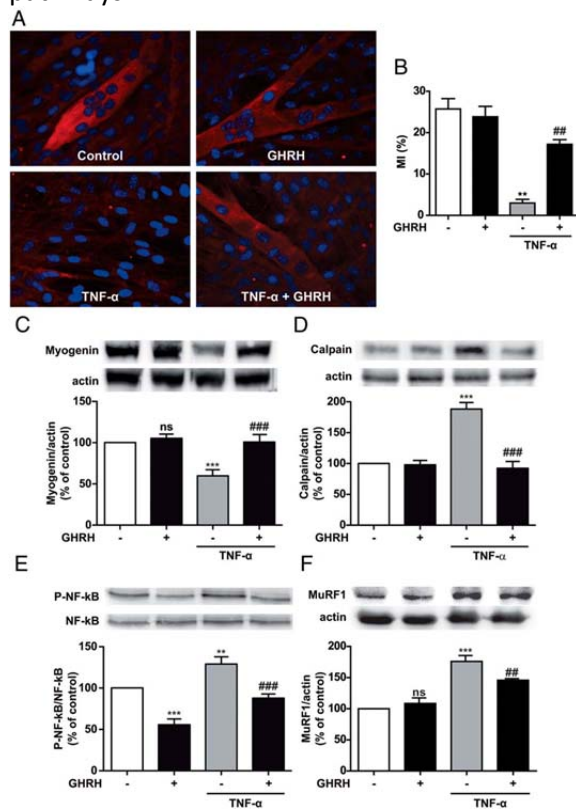
C2C12 cells were differentiated for 4 days in DM and then incubated for 48 hours in fresh DM in the absence or presence of 0.5 μM GHRH and either without or with TNF-α (20 ng/mL). A, Representative photomicrographs showing immunofluorescence staining for MyHC (red) and for nuclei, counterstained with Hoechst 33258 (blue) (magnification, ×200). B, Myogenic index (MI) of fusion calculated in cells stained as for panel A from 10 randomly chosen microscopic fields. **, $P < .01$ vs untreated cells (−); [##], $P < .01$ vs TNF-α treatment alone (gray column) (n = 3). Western blot analysis (48 h) for myogenin (C), calpain (D), P-NF-κB (E), and MuRF1 (F) (upper panels). Blots, representative of three independent experiments, were reprobed with antibodies to actin (C, D, and F) or total NF-κB (E) (bottom panels). Graphs represent the densitometric analysis of the proteins normalized to actin (C, D, and F) or to NF-κB (E) and reported as a percentage of control (untreated cells) (n = 3). **, $P < .01$, ***, $P < .001$ (ns, not significant) vs untreated (white columns); ##, $P < .01$, ###, $P < .001$ vs TNF-α (gray columns).

We then analyzed the expression of myogenin, a transcription factor essential for muscle cell differentiation and maintenance of differentiated state (29, 30). TNF-α caused a remarkable reduction of myogenin, whereas GHRH restored myogenin expression to basal level (Figure 6C).

Calpain proteolytic pathways are activated in atrophying muscle and play a major role in myofibrillar protein degradation (31). Furthermore, TNF-α has been shown to promote muscle wasting through activation of both calpain and the transcription factor NF-κB (5, 29, 32). Here TNF-α strongly stimulated calpain protein increase with respect to control, whereas GHRH completely blocked this effect (Figure 6D). Furthermore, TNF-α increased NF-κB phosphorylation, which was restored to control levels by cotreatment with GHRH. GHRH alone also strongly reduced phosphorylated NF-κB, compared with untreated cells (Figure 6E). Similarly, GHRH counteracted the TNF-α-induced increase of the atrophy-related E3 ubiquitin ligase MuRF1 (33), having no effect when administered alone (Figure 6F). Collectively these results suggest that GHRH counteracts TNF-α-induced myofibril degradation and activation of proteolytic pathways in C2C12 myotubes.

Discussion

This study shows that GHRH promotes survival and prevents apoptosis of C2C12 myotubes treated with TNF-α. These effects, which required GHRH binding to its receptor, involved activation of PI3K/Akt and

inactivation of GSK3-β pathways. Furthermore, GHRH prevented the TNF-α-induced reduction of myofibrillary proteins and activation of proteolytic pathways.

Skeletal muscle atrophy is a debilitating phenomenon, characteristic of many chronic diseases such as cancer, aging, diabetes, and heart failure (1–3). The proinflammatory cytokine TNF-α has been found elevated in these pathological states, strongly contributing to muscle wasting by inhibiting myogenesis and inducing apoptotic and proteolytic pathways in muscle cells (4, 6, 7, 25, 29, 34). Therefore, identification of compounds able to counteract cytokine-induced detrimental effects would lead to novel approaches for treating muscle atrophy. For such purpose, we considered GHRH an ideal candidate because of its survival action in many cell types and, particularly, because of its recently reported protective effects in both isolated cardiac myocytes and the whole heart (12–14, 16, 17, 35).

In addition to the hypothalamus, GHRH and GHRH-R are expressed in different rodent and human extrapituitary tissues (36–38). Furthermore, we and others have shown the presence of the hormone and its receptor in isolated cardiac myocytes and the heart (12, 14, 15, 36, 37), whereas expression in skeletal muscle has been described only in rats (36, 37). Aside from pituitary GHRH-R, GHRH-R splice variants have been shown in extrapituitary rodent and human tissues, and, particularly, in cancer cell lines and tumors (37–39). Here we first show that both GHRH and pituitary GHRH-R mRNA and protein are expressed in C2C12 myoblasts as well as during their differentiation and in myotubes, whereas the splice variant-1 isoform was undetectable, in line with previous findings in mouse muscle (37). Furthermore, expression of GHRH-R and GHRH mRNA was also found in both mouse soleus muscle and human rectus abdominis muscle, suggesting the potential importance of the hormone and its receptor in skeletal tissue growth and function. Interestingly, GHRH-R mRNA, and both GHRH and GHRH-R protein increased during C2C12 differentiation, suggesting an autocrine/paracrine role of the hormone in myogenesis and myotube survival. In this study, however, we did not specifically consider myogenesis, being focused on GHRH effects in differentiated myotubes. Indeed, to date, the potential effect of the hormone on skeletal muscle cell survival has not been investigated. Of note, Pommier et al (40) previously reported that GHRH increased muscle mass and reduced fat mass on the carcass of pigs by increasing protein content, suggesting anabolic effects in skeletal muscle. However, the underlying mechanisms were not investigated and activation of GH/IGF-I axis was proposed to be involved.

Here we first show the direct role of GHRH in C2C12 myotubes. TNF-α has been shown to promote muscle atrophy through mechanisms that include inhibition of myogenesis and induction of apoptosis in both myoblasts and myotubes (4, 6, 7, 25, 29, 34). Interestingly, TNF-α-induced proapoptotic effects in muscle were initially found only in myoblasts and differentiating myotubes but not in differentiated myotubes (6, 25, 41, 42). More recently, however, apoptotic effects in differentiated myotubes in vitro and in skeletal muscle in vivo were demonstrated (29, 43, 44). In the present study, we tested increasing concentrations of TNF-α in either differentiating myoblasts or myotubes and, in both conditions, evaluated cell survival and apoptosis at the end of differentiation. In line with previous findings (6, 25, 42), 20 ng/mL was the best concentration to reduce cell survival and promote apoptosis and was selected for the subsequent experiments. Similarly, 0.5 µM was chosen as the best GHRH concentration to counteract the harmful effects of TNF-α, in agreement with our previous findings in cardiac myocytes (12). We show that GHRH increased survival and reduced apoptosis in myotubes, when given to both differentiating or differentiated cells and to a similar extent, suggesting protective effects during both myogenesis and in mature myotubes. Interestingly, GHRH also blocked TNF-α-induced reduction of the antiapoptotic protein Bcl-2 and strongly up-regulated Bcl-2 expression, even in the absence of the cytokine, in line with its antiapoptotic role. Moreover, treatment with TNF-α reduced GHRH mRNA but not GHRH-R levels in C2C12 myotubes, suggesting that exogenous GHRH may indeed be needed to rescue muscle cells upon stress conditions such as inflammation during atrophy.

GHRH antagonists have been shown to inhibit GHRH actions in different cell types by binding to GHRH-R, indicating receptor-mediated mechanisms of the hormone (12, 13, 26). Moreover, in addition to suppressing pituitary GH/hepatic IGF-I in oncological patients, GHRH antagonists exert direct inhibitory

effects on cell proliferation and survival and on tumor growth (20, 26). Accordingly, the GHRH antagonist JV-1–36 was found here to abolish GHRH survival and antiapoptotic actions in both untreated and TNF-α-treated myotubes, in line with its previously observed receptor-mediated mechanisms. The involvement of GHRH-R in GHRH-induced myotube protection was further supported by evidence that JV-1–36 even prevented GHRH ability to counteract TNF-α-induced reduction of both Akt and GSK3-β phosphorylation.

GHRH effect on GH/IGF-I production in C2C12 myotubes was not investigated in this study. In fact, GH/IGF-I mRNA expression and secretion were recently shown in C2C12 differentiating cells along with autocrine antiapoptotic effects (45); moreover, GH administration in vivo was found to stimulate IGF-1 expression in skeletal muscle, suggesting GH/IGF-1-mediated autocrine/paracrine mechanisms of postnatal growth (46). Similarly, GH-induced IGF-1 mRNA was demonstrated in C2C12 cells (47); however, to date there is no evidence of GHRH effect on GH/IGF-1 expression in skeletal muscle. Interestingly, the synthetic GH secretagogue receptor agonist GH-releasing peptide-2, which, like ghrelin and GHRH, in some studies was shown to stimulate GH and IGF-1 secretion in vivo (48), increased IGF-1 levels neither in mice nor GH and IGF-1 expression in C2C12 cells (49). Therefore, in line with these findings and with our present results showing that GHRH does not activate the mTOR complex 1 (TORC1)/p70S6K, which is normally induced by IGF-1 in muscle cells (3), we suggest direct actions of GHRH in C2C12 myotubes. The possibility of other indirect mechanisms, however, cannot be excluded, and requires further investigation. In addition, whether GH exerts protective effects in skeletal muscle remains controversial, and GH was found unable to prevent apoptosis or increase viability in C2C12 and L6C5 myoblasts (50). Conversely, direct cardioprotective effects of GHRH and GHRH analogs in vitro and in vivo, not involving GH/IGF-1, have been recently demonstrated (12–15), whereas GH administration and increased IGF-1 levels were found ineffective and even caused adverse effects (14). Thus, a possible in vivo application for preventing muscle wasting and atrophy would be the use of GHRH analogs, which are more potent and longer-acting agents than native GHRH (51).

Cell viability and skeletal muscle mass are regulated by coordinated action of key regulatory pathways, such as PI3K/Akt and its downstream targets GSK-3β and mTOR/p70S6K (3). Indeed, PI3K/Akt inhibition, induced by agents such as inflammatory cytokines, leads to skeletal muscle atrophy, whereas its activation can suppress atrophy pathways (44, 52, 53). Accordingly, we found that TNF-α reduced Akt phosphorylation in C2C12 myotubes, whereas GHRH prevented this effect. Furthermore, GHRH alone increased the activation of Akt and the phosphorylation of GSK-3β, which becomes inactive and relieves inhibition onto the eukaryotic initiation factor 2B, thereby promoting translation initiation and protein synthesis (3). Interestingly, the PI3K inhibitor wortmannin not only blocked GHRH-induced phosphorylation of PI3K/Akt and GSK-3β in TNF-α-treated cells but also prevented the survival and antiapoptotic actions of the hormone, suggesting a key role for PI3K/Akt-GSK-3β in GHRH-protective effects. Conversely, GHRH was unable to activate TORC1 and mTOR/p70S6K, the other downstream target of PI3K/Akt involved in muscle protein synthesis and myotube hypertrophy (3, 18). These results were strengthened by the finding that rapamycin, a specific mTOR inhibitor, had no effect on GHRH-induced survival in TNF-α-treated myotubes, suggesting that GHRH does not activate TORC1/p70S6K and likely signals through the rapamycin-insensitive TORC2, which contributes to Akt activation as a feedback loop (3). Accordingly, Akt-induced phosphorylation and inhibition of GSK-3β were previously found to occur independently of mTOR, suggesting that Akt may independently activate one pathway or the other (54).

GSK-3β functions in skeletal muscle are not restricted to regulation of protein synthesis, and muscle-specific ablation of GSK-3β was recently found to accelerate regeneration of atrophied skeletal muscle (55). In fact, GSK-3β also controls expression of atrogin-1 and MuRF1, which are rate-limiting enzymes of UPS-mediated protein breakdown and are induced by many atrophy stimuli (3). Absence of GSK-3β also results in the sparing of myofibrillar proteins and myotube size during atrophy (56). NF-κB, in turn, is an essential mediator of TNF-α-induced catabolism and apoptosis in muscle cells, and increased NF-κB activity is responsible for the up-regulation of MuRF1 and atrogin-1, with increased activity of UPS and degradation of cytoskeletal proteins (2, 32, 33). Interestingly, increased PI3K/Akt activity has been shown to block MuRF1 and muscle atrophy F-Box increase by phosphorylating and inhibiting the Forkhead box O family of transcription factors during muscle atrophy (52, 57). Consistently, GHRH was found here to both increase

Akt signaling and to prevent TNF-α-induced increase of NF-κB and MuRF1, suggesting a role in preventing proteolytic degradation of muscle proteins. MuRF1 also physically binds and ubiquinates MyHC, and MuRF1 knockdown was found to increase MyHC, indicating that MuRF1 induces muscle atrophy at least in part by causing proteolysis of myosin proteins (1–3). Importantly, GHRH, in addition to reducing MuRF1, also restored MyHC expression in myotubes as well as the normal tubular morphology, that were both lost by TNF-α treatment. Expression of myogenin, a muscle-specific transcription factor involved in myogenesis and muscle repair (29, 30), was also restored by GHRH in TNF-α-treated myotubes, suggesting that GHRH also promotes muscle regeneration by inducing myogenic processes.

Protein loss during atrophy, besides the proteolytic systems, is also caused by activation of the cytosolic calcium-dependent calpain system. In fact, in sepsis-induced muscle wasting, increased serum levels of TNF-α correlated with a deregulation of intracellular calcium and a consequent activation of calpains (31). Calpains and the NF-κB-induced UPS are highly intertwined because calpain activation cleaves myofibrillar proteins, resulting in disruption of the sarcomere and release of myofilaments that are subsequently ubiquitinated and degraded by the proteasome. TNF-α was found here to strongly promote both NF-κB and calpain increase, confirming its pivotal role in proteolysis and muscle atrophy. As for MuRF1 and, even more potently, GHRH counteracted these effects by restoring both NF-κB and calpain to basal levels, further demonstrating its role against muscle wasting.

In summary, this study shows that GHRH, through receptor-mediated mechanisms, promotes skeletal muscle cell survival and prevents TNF-α-induced apoptosis and atrophy in myotubes by activating survival and myogenic pathways and inhibiting catabolic and proteolytic systems. Together with the previously observed cardioprotective effects, these findings provide new insight into the biological functions of GHRH and suggest a novel therapeutic role for the hormone in diseases associated with skeletal muscle atrophy.

Abbreviations:

DM   differentiation medium
GHRH-R   GHRH receptor
GSK-3β   glycogen synthase kinase-3β
MI   myogenic index of fusion
mTOR   mammalian target of rapamycin
MTT   3-(4,5-dimethylthiazol-2-yl)-2,5-diphenyltetrazolium bromide
MuRF1   muscle ring finger 1
MyHC   myosin heavy chain
NF-κB   nuclear factor-κB
P   phosphorylated
PI3K   phosphoinositide-3 kinase
p70S6K   p70 ribosomal S6 kinase
TORC1   mTOR complex 1
UPS   ubiquitin-proteasome system.

References

1. Schiaffino S, Dyar KA, Ciciliot S, Blaauw B, Sandri M. Mechanisms regulating skeletal muscle growth and atrophy. FEBS J. 2013;280:4294–4314
2. Kandarian SC, Jackman RW. Intracellular signaling during skeletal muscle atrophy. Muscle Nerve. 2006;33:155–165

3. Egerman MA, Glass DJ. Signaling pathways controlling skeletal muscle mass. Crit Rev Biochem Mol Biol. 2014;49:59–68

4. Cai D, Frantz JD, Tawa NE Jr, et al. IKKβ/NF-κB activation causes severe muscle wasting in mice. Cell. 2004;119:285–298

5. Bakkar N, Guttridge DC. NF-κB signaling: a tale of two pathways in skeletal myogenesis. Physiol Rev. 2010;90:495–511

6. Magee P, Pearson S, Allen J. The omega-3 fatty acid, eicosapentaenoic acid (EPA), prevents the damaging effects of tumour necrosis factor (TNF)-α during murine skeletal muscle cell differentiation. Lipids Health Dis. 2008;7:24

7. Li YP, Schwartz RJ, Waddell ID, Holloway BR, Reid MB. Skeletal muscle myocytes undergo protein loss and reactive oxygen-mediated NF-κB activation in response to tumor necrosis factor α. FASEB J. 1998;12:871–880

8. Guillemin R. Hypothalamic hormones a.k.a. hypothalamic releasing factors. J Endocrinol. 2005;184:11–28

9. Kiaris H, Chatzistamou I, Papavassiliou AG, Schally AV. Growth hormone-releasing hormone: not only a neurohormone. Trends Endocrinol Metab. 2011;22:311–317

10. Frohman LA, Kineman RD. Growth hormone-releasing hormone and pituitary development, hyperplasia and tumorigenesis. Trends Endocrinol Metab. 2002;13:299–303

11. Pombo CM, Zalvide J, Gaylinn BD, Dieguez C. Growth hormone-releasing hormone stimulates mitogen-activated protein kinase. Endocrinology. 2000;141:2113–2119

12. Granata R, Trovato L, Gallo MP, et al. Growth hormone-releasing hormone promotes survival of cardiac myocytes in vitro and protects against ischaemia-reperfusion injury in rat heart. Cardiovasc Res. 2009;83:303–312

13. Penna C, Settanni F, Tullio F, et al. GH-releasing hormone induces cardioprotection in isolated male rat heart via activation of RISK and SAFE pathways. Endocrinology. 2013;154:1624–163514. Kanashiro-Takeuchi RM, Tziomalos K, Takeuchi LM, et al. Cardioprotective effects of growth hormone-releasing hormone agonist after myocardial infarction. Proc Natl Acad Sci USA. 2010;107:2604–260915. Bagno LL, Kanashiro-Takeuchi RM, Suncion VY, et al. Growth hormone-releasing hormone agonists reduce myocardial infarct scar in swine with subacute ischemic cardiomyopathy. J Am Heart Assoc. 2015;4

16. Kanashiro-Takeuchi RM, Takeuchi LM, Rick FG, et al. Activation of growth hormone releasing hormone (GHRH) receptor stimulates cardiac reverse remodeling after myocardial infarction (MI). Proc Natl Acad Sci USA. 2012;109:559–563

17. Florea V, Majid SS, Kanashiro-Takeuchi RM, et al. Agonists of growth hormone-releasing hormone stimulate self-renewal of cardiac stem cells and promote their survival. Proc Natl Acad Sci USA. 2014;111:17260–1726518. Rommel C, Bodine SC, Clarke BA, et al. Mediation of IGF-1-induced skeletal myotube hypertrophy by PI(3)K/Akt/mTOR and PI(3)K/Akt/GSK3 pathways. Nat Cell Biol. 2001;3:1009–1013

19. Granata R, Gallo D, Luque RM, et al. Obestatin regulates adipocyte function and protects against diet-induced insulin resistance and inflammation. FASEB J. 2012;26(8):3393–341120. Annunziata M, Grande C, Scarlatti F, et al. The growth hormone-releasing hormone (GHRH) antagonist JV-1–36 inhibits proliferation and survival of human ectopic endometriotic stromal cells (ESCs) and the T HESC cell line. Fertil Steril. 2010;94:841–849

21. Granata R, Settanni F, Trovato L, et al. RFamide peptides 43RFa and 26RFa both promote survival of pancreatic β-cells and human pancreatic islets but exert opposite effects on insulin secretion. Diabetes. 2014;63:2380–2393

22. Walsh K, Perlman H. Cell cycle exit upon myogenic differentiation. Curr Opin Genet Dev. 1997;7:597–602

23. Dirks AJ, Leeuwenburgh C. Tumor necrosis factor α signaling in skeletal muscle: effects of age and caloric restriction. J Nutr Biochem. 2006;17:501–508

24. Langen RC, Schols AM, Kelders MC, Wouters EF, Janssen-Heininger YM. Inflammatory cytokines inhibit myogenic differentiation through activation of nuclear factor-κB. FASEB J. 2001;15:1169–1180

25. Miller SC, Ito H, Blau HM, Torti FM. Tumor necrosis factor inhibits human myogenesis in vitro. Mol Cell Biol. 1988;8:2295–2301

26. Schally AV, Varga JL, Engel JB. Antagonists of growth-hormone-releasing hormone: an emerging new therapy for cancer. Nat Clin Pract Endocrinol Metab. 2008;4:33–43

27. Manning BD, Cantley LC. AKT/PKB signaling: navigating downstream. Cell. 2007;129:1261–1274

28. Buck M, Chojkier M. Muscle wasting and dedifferentiation induced by oxidative stress in a murine model of cachexia is prevented by inhibitors of nitric oxide synthesis and antioxidants. EMBO J. 1996;15:1753–1765

29. Tolosa L, Morla M, Iglesias A, Busquets X, Llado J, Olmos G. IFN-γ prevents TNF-α-induced apoptosis in C2C12 myotubes through down-regulation of TNF-R2 and increased NF-κB activity. Cell Signal. 2005;17:1333–1342

30. Cooper RN, Tajbakhsh S, Mouly V, Cossu G, Buckingham M, Butler-Browne GS. In vivo satellite cell activation via Myf5 and MyoD in regenerating mouse skeletal muscle. J Cell Sci. 1999;112(Pt 17):2895–2901

31. Smith IJ, Lecker SH, Hasselgren PO. Calpain activity and muscle wasting in sepsis. Am J Physiol Endocrinol Metab. 2008;295:E762–E771

32. Andrianjafiniony T, Dupre-Aucouturier S, Letexier D, Couchoux H, Desplanches D. Oxidative stress, apoptosis, and proteolysis in skeletal muscle repair after unloading. Am J Physiol Cell Physiol. 2010;299:C307–C315

33. Bodine SC, Latres E, Baumhueter S, et al. Identification of ubiquitin ligases required for skeletal muscle atrophy. Science. 2001;294:1704–1708

34. Schakman O, Dehoux M, Bouchuari S, et al. Role of IGF-I and the TNFα/NF-κB pathway in the induction of muscle atrogenes by acute inflammation. Am J Physiol Endocrinol Metab. 2012;303:E729–E739.

35. Granata R, Isgaard J, Alloatti G, Ghigo E. Cardiovascular actions of the ghrelin gene-derived peptides and growth hormone-releasing hormone. Exp Biol Med (Maywood). 2011;236:505–514.

36. Matsubara S, Sato M, Mizobuchi M, Niimi M, Takahara J. Differential gene expression of growth hormone (GH)-releasing hormone (GRH) and GRH receptor in various rat tissues. Endocrinology. 1995;136:4147–4150

37. Christodoulou C, Schally AV, Chatzistamou I, et al. Expression of growth hormone-releasing hormone (GHRH) and splice variant of GHRH receptors in normal mouse tissues. Regul Pept. 2006;136:105–108.

38. Havt A, Schally AV, Halmos G, et al. The expression of the pituitary growth hormone-releasing hormone receptor and its splice variants in normal and neoplastic human tissues. Proc Natl Acad Sci USA. 2005;102:17424–17429.

39. Barabutis N, Schally AV. Growth hormone-releasing hormone: extrapituitary effects in physiology and pathology. Cell Cycle. 2010;9:4110–4116.

40. Pommier SA, Dubreuil P, Pelletier G, Gaudreau P, Mowles TF, Brazeau P. Effect of a potent analog of human growth hormone-releasing factor on carcass composition and quality of crossbred market pigs. J Anim Sci. 1990;68:1291–1298.

41. Li YP, Reid MB. NF-κB mediates the protein loss induced by TNF-α in differentiated skeletal muscle myotubes. Am J Physiol Regul Integr Comp Physiol. 2000;279:R1165–R1170.

42. Chen S, Guttridge DC, Tang E, Shi S, Guan K, Wang CY. Suppression of tumor necrosis factor-mediated apoptosis by nuclear factor κB-independent bone morphogenetic protein/Smad signaling. J Biol Chem. 2001;276:39259–39263.

43. Phillips T, Leeuwenburgh C. Muscle fiber specific apoptosis and TNF-α signaling in sarcopenia are attenuated by life-long calorie restriction. FASEB J. 2005;19:668–670.

44. Sishi BJ, Engelbrecht AM. Tumor necrosis factor α (TNF-α) inactivates the PI3-kinase/PKB pathway and induces atrophy and apoptosis in L6 myotubes. Cytokine. 2011;54:173–184.

45. Segard HB, Moulin S, Boumard S, Augier de Cremiers C, Kelly PA, Finidori J. Autocrine growth hormone production prevents apoptosis and inhibits differentiation in C2C12 myoblasts. Cell Signal. 2003;15:615–623.

46. Isgaard J, Nilsson A, Vikman K, Isaksson OG. Growth hormone regulates the level of insulin-like growth factor-I mRNA in rat skeletal muscle. J Endocrinol. 1989;120:107–112.

47. Sadowski CL, Wheeler TT, Wang LH, Sadowski HB. GH regulation of IGF-I and suppressor of cytokine signaling gene expression in C2C12 skeletal muscle cells. Endocrinology 2001;142:3890–3900.

48. Bowers CY, Granda R, Mohan S, Kuipers J, Baylink D, Veldhuis JD. Sustained elevation of pulsatile growth hormone (GH) secretion and insulin-like growth factor I (IGF-I), IGF-binding protein-3 (IGFBP-3), and IGFBP-5 concentrations during 30-day continuous subcutaneous infusion of GH-releasing peptide-2 in older men and women. J Clin Endocrinol Metab. 2004;89:2290–2300.

49. Yamamoto D, Ikeshita N, Matsubara T, et al. GHRP-2, a GHS-R agonist, directly acts on myocytes to attenuate the dexamethasone-induced expressions of muscle-specific ubiquitin ligases, Atrogin-1 and MuRF1. Life Sci. 2008;82:460–466.

50. Dimauro I, Magi F, La Sala G, Pittaluga M, Parisi P, Caporossi D. Modulation of the apoptotic pathway in skeletal muscle models: the role of growth hormone. Growth Factors. 2011;29:21–35.

51. Cai R, Schally AV, Cui T, et al. Synthesis of new potent agonistic analogs of growth hormone-releasing hormone (GHRH) and evaluation of their endocrine and cardiac activities. Peptides. 2014;52:104–112.

52. Stitt TN, Drujan D, Clarke BA, et al. The IGF-1/PI3K/Akt pathway prevents expression of muscle atrophy-induced ubiquitin ligases by inhibiting FOXO transcription factors. Mol Cell. 2004;14:395–403.

53. Bodine SC, Stitt TN, Gonzalez M, et al. Akt/mTOR pathway is a crucial regulator of skeletal muscle hypertrophy and can prevent muscle atrophy in vivo. Nat Cell Biol. 2001;3:1014–1019.

54. Cross DA, Alessi DR, Cohen P, Andjelkovich M, Hemmings BA. Inhibition of glycogen synthase kinase-3 by insulin mediated by protein kinase B. Nature. 1995;378:785–789.

55. Pansters NA, Schols AM, Verhees KJ, et al. Muscle-specific GSK-3β ablation accelerates regeneration of disuse-atrophied skeletal muscle. Biochim Biophys Acta. 2014;1852:490–506.

56. Verhees KJ, Schols AM, Kelders MC, Op den Kamp CM, van der Velden JL, Langen RC. Glycogen synthase kinase-3β is required for the induction of skeletal muscle atrophy. Am J Physiol Cell Physiol. 2011;301:C995–C1007.

57. Sandri M, Sandri C, Gilbert A, et al. Foxo transcription factors induce the atrophy-related ubiquitin ligase atrogin-1 and cause skeletal muscle atrophy. Cell. 2004;117:399–412.